Title

A Fine Balance of Dietary Lipids Improves Pathology of a Murine Model of VCP-Associated Multisystem Proteinopathy

Journal

PLOS ONE, 10(7)

ISSN

1932-6203

Authors

Llewellyn, Katrina J
Walker, Naomi
Nguyen, Christopher
et al.

Publication Date

2015

DOI

10.1371/journal.pone.0131995

Peer reviewed

PLOS | ONE

RESEARCH ARTICLE

A Fine Balance of Dietary Lipids Improves Pathology of a Murine Model of VCP-Associated Multisystem Proteinopathy

Katrina J. Llewellyn[1,2], Naomi Walker[1], Christopher Nguyen[1], Baichang Tan[1], Lbachir BenMohamed[3,4], Virginia E. Kimonis[1,2], Angèle Nalbandian[1,2]*

1 Department of Pediatrics, Division of Genetics and Genomics Medicine, University of California Irvine, Irvine, CA, 92697, United States of America, **2** Sue and Bill Gross Stem Institute, University of California Irvine, Irvine, CA, 92697, United States of America, **3** Laboratory of Cellular and Molecular Immunology, Gavin Herbert Eye Institute, University of California Irvine, School of Medicine, Irvine, CA, 92697, United States of America, **4** Institute for Immunology, University of California Irvine, School of Medicine, Irvine, CA, 92697, United States of America

* a.nalbandian@uci.edu

OPEN ACCESS

Citation: Llewellyn KJ, Walker N, Nguyen C, Tan B, BenMohamed L, Kimonis VE, et al. (2015) A Fine Balance of Dietary Lipids Improves Pathology of a Murine Model of VCP-Associated Multisystem Proteinopathy. PLoS ONE 10(7): e0131995. doi:10.1371/journal.pone.0131995

Editor: Udai Pandey, Children's Hospital of Pittsburgh, University of Pittsburgh Medical Center, UNITED STATES

Received: February 18, 2015

Accepted: June 9, 2015

Published: July 2, 2015

Data Availability Statement: All relevant data are within the paper.

Funding: This work was supported by National Institutes of Health (NIH) grant R21 AR063360 and Muscular Dystrophy Association (MDA) 175682. The funders had no role in study design, data collection and analysis, decision to publish, or preparation of the manuscript.

Competing Interests: The authors have declared that no competing interests exist.

Abstract

The discovery of effective therapies and of disease mechanisms underlying valosin containing protein (VCP)-associated myopathies and neurodegenerative disorders remains elusive. VCP disease, caused by mutations in the *VCP* gene, are a clinically and genetically heterogeneous group of disorders with manifestations varying from hereditary inclusion body myopathy, Paget's disease of bone, frontotemporal dementia (IBMPFD), and amyotrophic lateral sclerosis (ALS). In the present study, we examined the effects of higher dietary lipid percentages on $VCP^{R155H/R155H}$, $VCP^{R155H/+}$ and Wild Type (WT) mice from birth until 15 months of age by immunohistochemical and biochemical assays. Findings illustrated improvement in the muscle strength, histology, and autophagy signaling pathway in the heterozygote mice when fed 9% lipid-enriched diets (LED). However, increasing the LED by 12%, 30%, and 48% showed no improvement in homozygote and heterozygote survival, muscle pathology, lipid accumulation or the autophagy cascade. These findings suggest that a balanced lipid supplementation may have a therapeutic strategy for patients with VCP-associated multisystem proteinopathies.

Introduction

Inclusion body myopathy associated with Paget's disease of bone, and frontotemporal dementia (IBMPFD), more recently termed multisystem proteinopathy (MSP), is a progressive, fatal genetic disorder caused by mutations in the *VCP* gene [1]. Predominantly, affected individuals exhibit scapular winging and progressive muscle weakness and die from cardiac and respiratory failures [1–4]. Patients may demonstrate a mixture of the three phenotypes or just one phenotype in isolation. Myopathy is the most common feature, present in nearly ninety percent of affected individuals with patients typically depicting weakness and atrophy of skeletal,

pelvic and shoulder girdle muscles [2, 5]. Rimmed vacuoles and TAR DNA Binding Protein-43 (TDP-43)-positive ubiquitinated inclusion bodies are hallmarks in IBMPFD patients' muscles [2, 5, 6, 7].

To date, over 31 mutations in the *VCP* gene have been identified, with IBMPFD having been reported in more than 39 families worldwide [8]. Linkage studies have localized the IBMPFD gene mutation to VCP on chromosome 9p21.1-p12. The most common mutation is the R155H accounting for approximately 50% of affected individuals. Our IBMPFD patients' myoblasts have shown impairment in the autophagy transduction cascade [9, 10]. More recently, global microarray analyses in patients quadriceps muscles have demonstrated the association of IBMPFD disease with several signaling transduction pathways including abnormalities in the actin cytoskeleton, ErbB signaling, cancer, regulation of autophagy and lysosomal signaling transduction cascades [11].

Recently, VCP has been implicated at the intersection of the autophagy, a multi-step mechanism responsible for degrading and recycling defective organelles and maintaining cellular homeostasis [1]. Inhibition of this process plays a critical role in the pathogenesis of several inherited myopathies [12]. Impaired autophagic degradation is thought to contribute to Alzheimer's and Huntington's diseases, among other neurodegenerative diseases, as well as in inflammatory disorders [13, 14]. In addition, several studies have shown the involvement of impaired autophagic degradation in the pathogenesis of other human myopathies such as Pompe disease [15] and sporadic inclusion body myositis (sIBM) [16].

Our heterozygous $VCP^{R155H/+}$ mouse model at 12-months of age with the common disease-related R155H *VCP* mutation mimics human VCP-associated myopathy, including progressive muscle, bone, spinal cord and brain pathology [17, 18]. We developed the R155H homozygous ($VCP^{R155H/R155H}$) mouse model to provide a rapid mouse model exhibiting progressive muscle weakness starting from birth and accelerated pathology including in muscle, spinal cord, brain, and heart muscles[19]. This unique model has provided a significant advancement in the understanding of the underlying pathophysiological mechanisms in the hopes of discovering effective and safe therapeutic strategies to treat VCP disease [20].

Our previous findings reported on feeding 9% lipid-enriched diet (LED) to pregnant heterozygous $VCP^{R155H/+}$ dams produced large litters of homozygous $VCP^{R155H/R155H}$ offspring that appeared healthy, active, and lived longer, for several months, compared to the maximum 21 day survival observed in mice fed a normal chow [21]. In this report, we first investigated the beneficial effects of the 9% lipid-enriched diet on the heterozygote $VCP^{R155H/+}$ mice, as they have the R155H mutation on one allele, the same genetic mutation as patients suffering with VCP-associated disease. We found that the 9% lipid-enriched diet had a significant beneficial effect on the pathology in heterozygote $VCP^{R155H/+}$ mice, with improved muscle strength and architecture as well as decreased expression of autophagy markers, LC3 and p62/*SQSTM1*. The benefit was most apparent with early intervention. Secondly, we investigated whether increasing the lipid diets to 12%, 30%, and 48% would further slowdown the progression of VCP-associated disease, offering a novel treatment strategy. However, our results showed no improvement in survival, muscle pathology or the autophagy cascade with these increased lipid diets. Therefore, these findings suggest that balanced lipid supplementation may offer a promising therapeutic option for patients with VCP-associated neurodegenerative diseases.

Materials and Methods

Ethics Statement and Animal Models

This study was carried out in strict accordance with the recommendations and procedures outlined in the Guide for the Care and Use of Laboratory Animals of the National Institutes of

Health under Assurance Number A3873-1. Experiments were conducted with the approval of the Institutional Animal Care and Use Committee (*IACUC Protocol #2007-2716-2*) of University of California-Irvine (Irvine, CA). All efforts were made to minimize suffering. Animals were housed at the University of California-Irvine vivarium and maintained as previously described [21]. Mouse genotyping was performed at Transnetyx Inc. (Cordova, TN).

Animal Diet Regimens

$VCP^{R155H/+}$ heterozygote pregnant dams were chosen for this study and placed on the *ad libitum* lipid-enriched diet (2019X Teklad Rodent Diets, Harlan Laboratories Inc., Madison, WI) (9%, 12%, 30%, and 48% LED) or standard normal diet (2020X). At weaning, the heterozygotes ($VCP^{R155H/+}$), homozygotes ($VCP^{R155H/R155H}$), and Wild Type (WT) mice were separated and continued to receive the same diet. Mice were genotyped as previously described [21].

Grip Strength and Rotarod Measurement Studies

Muscle strength of the forelimbs of $VCP^{R155H/+}$ and WT animals on the normal diet (6%) and LED (9%, 12%, 30%, and 48%) were measured on at 6–12- and 15- months using a Grip Strength Meter apparatus (TSE Systems Gmbh, Hamburg, Germany) as described previously [22].

To assess Rotarod performance measurements, $VCP^{R155H/+}$ and WT animals on the normal diet and LED (9%, 12%, 30%, and 48%) were measured at 15- months of age. Mice were placed on the Rotarod apparatus, which was set to accelerate from 4 to 40 rpm in 5 minutes. Mice performed three trials with 45-minute to 60-minute intertrial intervals on each of two consecutive days.

Histological Analyses

Fifteen month old WT and $VCP^{R155H/+}$ quadriceps muscles were harvested. Hematoxylin and Eosin staining was performed and analyzed by light microscopy (Carl Zeiss, Thornwood, NY). Oil Red O staining was performed on the mice of varying diets (9%, 12%, 30% and 48%) using routine methods and analyzed by light microscopy (Carl Zeiss). For immunohistochemical analyses, sections were stained with TDP-43 (1:3,000 dilution; rabbit monoclonal anti-TDP-43 antibody Cat. No. #ab109535, Abcam, Cambridge, MA), p62/*SQSTM1* (1:5,000 dilution; rabbit polyclonal anti-*SQSTM1*/p62 antibody, Cat. No. #ab91526, Abcam, Cambridge, MA), and LC3-I/II (1:3,000 dilution; rabbit polyclonal anti-LC3 B antibody, Cat. No. #ab64781, Abcam, Cambridge, MA) and mounted as previously described [21].

Western Blot Analysis

Fifteen month old $VCP^{R155H/+}$ and WT quadriceps muscles were harvested and extracted using the NE-PER Nuclear and Cytoplasmic Extraction Kit (Thermo Scientific). Protein concentrations were determined using the Nanodrop and separated on Bis-Tris 4–12% NuPAGE gels (Invitrogen Life Technologies Inc., Carlsbad, CA). Expression levels of proteins were analyzed by Western blotting using ubiquitin (1:5,000 dilution; rabbit polyclonal anti-ubiquitin antibody, Cat. No. #ab7780, Abcam, Cambridge, MA), optineurin (1:5,000 dilution; rabbit polyclonal anti-optineurin antibody, Cat. No. #ab23666, Abcam, Cambridge, MA), p62/*SQSTM1* (1:5,000 dilution; rabbit polyclonal anti-*SQSTM1*/p62 antibody, Cat. No. #ab91526, Abcam, Cambridge, MA), TDP-43 (1:5,000 dilution; rabbit monoclonal anti-TDP-43 antibody Cat. No. #ab109535, Abcam, Cambridge, MA), LC3-I/II (1:3,000 dilution; rabbit polyclonal anti-LC3 B antibody, Cat. No. #ab64781, Abcam, Cambridge, MA), acid phosphatase (1:3,000

dilution; rabbit monoclonal anti-acid phosphatase antibody, Cat. No. #ab166896, Abcam, Cambridge, MA), and lysosomal acid lipase (LAL) (1:5,000 dilution; rabbit polyclonal anti-lysosomal acid lipase antibody, Cat. No. #ab154356, Abcam, Cambridge, MA), mucolipin-1 (TRPML1) (1:1,000 dilution; rabbit polyclonal anti-TRPML1-specific antibodies, Cat. No. ab74857 Abcam, Cambridge, MA). Equal protein loading was confirmed by β-actin antibodies (1:20,000 dilution; mouse monoclonal anti- β-actin antibody, Cat. No. #ab6277, Abcam, Cambridge, MA) staining. These antibodies were previously validated in our most recent publications [21, 23, 24]. These experiments are representative of triplicates.

Statistical Analysis

We compared the aforementioned studies—including grip strength and Rotarod performance studies, among normal diet and various lipid-enriched diet-fed $VCP^{R155H/+}$ and WT mice using mixed model analysis of variance (one-way ANOVA). We used the Kaplan-Meier curve analysis with log-rank tests ($P < 0.01$) for survival studies ($VCP^{R155H/R155H}$, $VCP^{R155H/+}$ and WT mice).

Results

$VCP^{R155H/+}$ heterozygotes mice fed 9% LED from birth illustrate no VCP disease pathology

To assess the short-term and long-term effects of LED, we performed histological analysis of quadriceps muscle in heterozygous $VCP^{R155H/+}$ and WT littermates. We placed the $VCP^{R155H/+}$ pregnant dams on a 9% LED from birth and monitored their survival as well as prevention of muscle pathology. Improved grip strength measurements were noted in the $VCP^{R155H/+}$ mice on the LED from birth in comparison to the $VCP^{R155H/+}$ mice on a normal diet (ND) (Fig 1A). Remarkably, the $VCP^{R155H/+}$ heterozygote animals showed delayed onset of pathology at later ages. We also placed $VCP^{R155H/+}$ mice on 9% LED at 7 months of age after a normal diet of 6% fat from birth and discovered that the diet was able to significantly prevent muscle pathology, however, less effectively than from birth (Fig 1B–1D). Western blot analyses of ubiquitin and LC3-I/II expression levels showed no significant changes in WT and $VCP^{R155H/+}$ on a 9% LED vs. ND starting at 7 months of age ($p > 0.05$, Fig 1E). Autophagy markers p62/SQSTM1 and TDP-43 (total fractions) showed slightly increased expression levels in $VCP^{R155H/+}$ mice after 7 months on 9% LED when compared to $VCP^{R155H/+}$ fed ND (Fig 1E). However, optineurin levels in the $VCP^{R155H/+}$ mice after 7 months on 9% LED showed a significant decrease when compared to $VCP^{R155H/+}$ fed ND ($p = 0.05$). No significant differences were observed between WT and heterozygotes on the ND vs. the 9% LED. Moreover, these Western blot results were confirmed using densitometry analyses (Fig 1F).

Survival rates for VCP heterozygotes and homozygotes mice fed on varying LEDs

We placed pregnant heterozygote dams on a lipid-enriched diet (2019X Teklad Global Rodent Diet) versus the normal diet (2020X Teklad Global Rodent Diet) and monitored the survival of the $VCP^{R155H/+}$, $VCP^{R155H/R155H}$ and WT offspring (Fig 2A, 2B and 2F). $VCP^{R155H/R155H}$ homozygous mice on a normal diet did not survive till weaning and were too weak for strength measurements ($p < 0.05$). The Kaplan-Meier survival rate amongst homozygous $VCP^{R155H/R155H}$ animals improved drastically on the 9% lipid-enriched diet versus their littermates on the normal diet ($p \leq 0.001$) (Fig 2B), however, the diet did not completely reverse the lethality. Survivals for the homozygous $VCP^{R155H/R155H}$ animals on higher LEDs significantly deteriorated

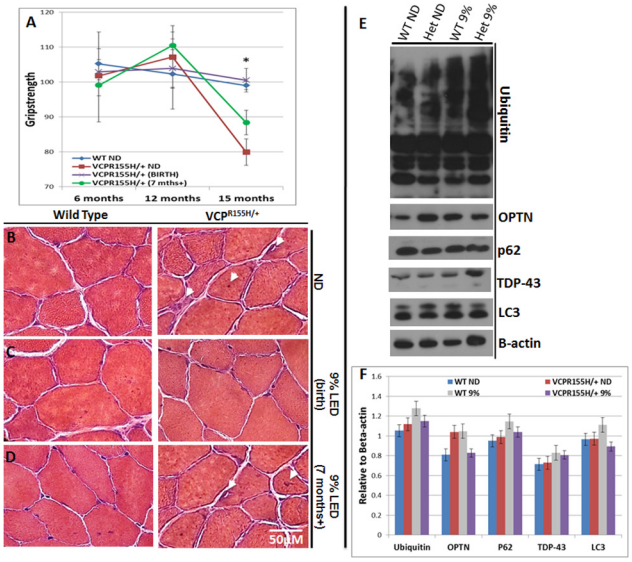

Fig 1. Grip strength measurements and histological analyses of WT and VCP$^{R155H/+}$ mice on normal and 9% LED. (A) Grip strength measurements for the WT (blue) and VCP$^{R155H/+}$ (red) mice placed on the 6% ND from birth and VCP$^{R155H/+}$ mice placed on the 9% LED from birth (purple) and at 7 months of age onwards (green). H&E staining on WT and VCP$^{R155H/+}$ on (B) ND (pathology shown by white arrows, right panel), (C) 9% LED from birth, and (D) 9% LED beginning at 7 months of age onwards (pathology shown by white arrows, right panel). (E) Western blot analyses of WT and VCP$^{R155H/+}$ animals fed either ND or 9% LED. (F) Densitometry analyses relative to loading control (Beta-actin). Statistical significance is denoted by *P $\leq$ 0.05.

doi:10.1371/journal.pone.0131995.g001

as higher LEDs were lethal; and therefore, they were not included for the remainder of the study (Fig 2C–2F, as shown in green). Pregnant dams did not produce large litters as was observed with the 9% LED, instead litters were small and produced very few or no VCP$^{R155H/R155H}$ homozygotes. There was no considerable difference in survival between age- and sex-matched WT and VCP$^{R155H/+}$ animals on the normal diet versus the 12% LED, however with

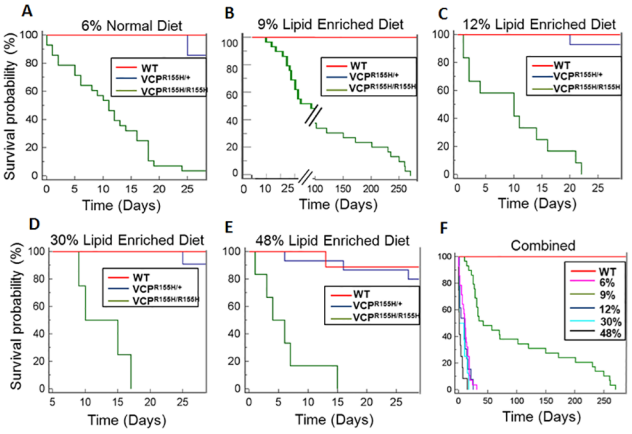

Fig 2. Survival curves of WT, VCP$^{R155H/+}$, and VCP$^{R155H/R155H}$ mice on normal and varying lipid-enriched diets. Kaplan-Meier survival probability (%) analysis for the WT, VCP$^{R155H/+}$, and VCP$^{R155H/R155H}$ pregnant dams placed on the (A) 6% normal diet, (B) 9% LED, (C) 12% LED, (D) 30% LED, and (E) 48% LED. (F) Combined survival curve of all the LED regimens for the WT, VCP$^{R155H/+}$, and VCP$^{R155H/R155H}$. The number of mice analyzed per experiment is 35–40.

doi:10.1371/journal.pone.0131995.g002

the 30% LED and 48% LED there was a significant drop in survival of homozygous $VCP^{R155H/R155H}$ and heterozygous $VCP^{R155H/+}$ mice (Fig 2C–2F, as shown in red and blue).

Increasing LEDs illustrate pathology and lipid droplets in $VCP^{R155H/+}$ heterozygotes mice

To evaluate the effects of varying percentages of LEDs, we analyzed grip strength and Rotarod performance measurements. Grip strength analyses of the $VCP^{R155H/+}$ mice on 30% and 48% revealed decreased strength while no differences were observed in 12% when compared to mice on the ND (Fig 3A). Rotarod performance measurements depicted decreased motor coordination in $VCP^{R155H/+}$ mice on 30% and 48% LED (Fig 3B).

Next, we performed histological analysis of quadriceps muscles in age- and sex-matched heterozygotes and WT littermates. By Hematoxylin and Eosin (H&E) staining, heterozygous $VCP^{R155H/+}$ mice on the increased LEDs (12%, 30%, and 48%) showed centrally localized nuclei, increased endomysial space between the muscle fibers, abnormal mitochondrial pathology and neurogenic changes, similar to patients with VCP-associated disease. These results were not seen in the heterozygous $VCP^{R155H/+}$ mice fed the 9% LED (Fig 3C and 3D, as shown by arrows and magnified insets).

Our previous study showed increased generation of lipid granules by Oil red O staining in our homozygous $VCP^{R155H/R155H}$ mice fed a 6% ND, which was corrected by the 9% LED.

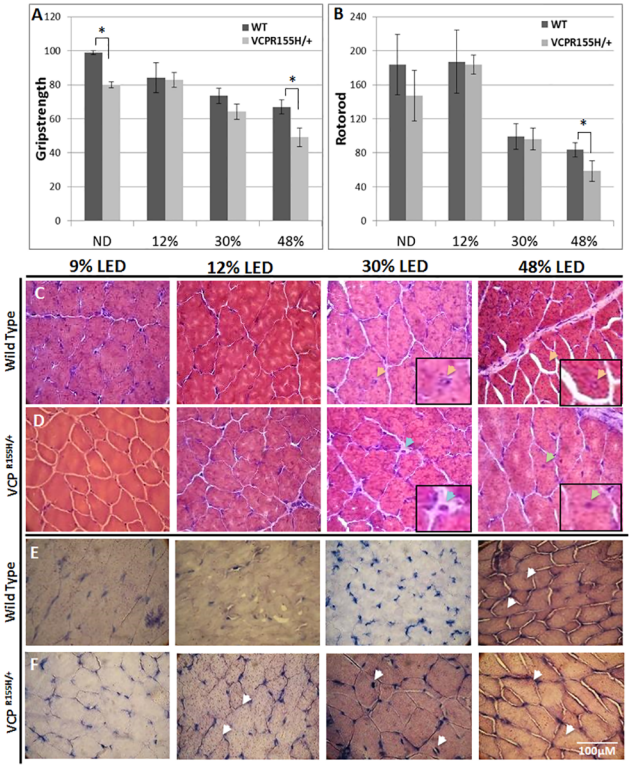

Fig 3. Strength measurements and histological stainings of quadriceps muscle of WT and $VCP^{R155H/+}$ mice on normal and different lipid-enriched diets. (A,B) Grip strength and Rotarod measurements analyses at 15-months of age, (C,D) H&E and (E,F) Oil Red O staining of quadriceps muscle from WT and $VCP^{R155H/+}$ animals placed on the 9%, 12%, 30%, and 48% LED from birth. The number of mice analyzed per experiment is 8–10. Insets show magnified pathology, including rimmed vacuoles (orange arrows), atrophy (blue arrows), centralized nuclei (green arrows), and increased lipid droplets (white arrows).

doi:10.1371/journal.pone.0131995.g003

Table 1. Percentage of macronutrients for each specific normal diet (ND) and lipid-enriched diet (LED).

Macronutrients (%)	Lipid	Carbohydrate	Crude Protein
6% ND	**6.5**	**62**	**19.1**
9% LED	**9.0**	**59.6**	**19.0**
12% LED	**12.2**	**55.3**	**17.7**
30% LED	**30.2**	**38.2**	**17.7**
48% LED	**48.2**	**21.3**	**17.7**

doi:10.1371/journal.pone.0131995.t001

Therefore, we analyzed Oil Red O staining in our heterozygous mice fed the varying LEDs. WT and $VCP^{R155H/+}$ mice on the 9% LED did not reveal lipid accumulation (Fig 3E and 3F). However, $VCP^{R155H/+}$ animals displayed progressive accumulation of lipid droplets in muscle quadriceps fibers on the increased LEDs (12%, 30%, and 48%) in comparison to our WT mice which showed no accumulation of lipid droplets apart from those fed the 30% and 48% LEDs (Fig 3E and 3F). Therefore, we hypothesize that feeding a balanced diet, including 9% lipids, 59.6% carbohydrate and 19% protein (Table 1) seems sufficient to normalize the lipid abnormalities, further highlighting their pathological relevance in VCP disease.

Autophagy flux in $VCP^{R155H/+}$ heterozygotes mice fed on increasing LEDs

Previously, we have identified a dysfunction in the autophagic signaling cascade via accumulation of autophagy intermediates, such as p62/*SQSTM1* and Light Chain LC3-I/II, in $VCP^{R155H/+}$ animals versus their WT littermates [19, 23]. To assess the effects of LEDs on $VCP^{R155H/+}$ animals versus their WT littermates, we monitored autophagy flux by detection of endogenous LC3-I/II modification, ubiquitin-positive and p62/*SQSTM1*-positive inclusions.

In comparison to the WT mice, the $VCP^{R155H/+}$ mice on increasing LED displayed comparable levels of ubiquitin, however, decreased levels of LC3-I and LC3-II protein expressions, as well as reduced levels in p62/*SQSTM1* protein (Fig 4D and 4E). Interestingly, magnified insets revealed increased p62 puncta aggregates in the heterozygous $VCP^{R155H/+}$ mice on the 30% and 48% LED, suggesting increased autophagy dysregulation, even though there was decreased levels of p62 overall (Fig 4A–4C, magnified insets). Furthermore, we examined the TDP-43 aggregates (nuclear to cytoplasmic translocation) in the $VCP^{R155H/+}$ animals versus their WT littermates and showed nuclear TDP-43 expression, suggestive of a reduced pathological phenotype (Fig 4A–4C, indicated by white arrows). Western blot and densitometry analyses of ubiquitin, LC3-I/II, p62/*SQSTM1*, and TDP-43 confirmed these findings (Fig 4D and 4E).

Our results indicate that increased percentages of LEDs had a detrimental effect in muscle pathology and expression of autophagy markers in $VCP^{R155H/+}$ mice. Overall, these results indicate that systemic alterations in lipid metabolism may underlie the muscle-specific pathology of $VCP^{R155H/+}$ mice.

Effects of varying LEDs on the expression of lysosomal enzymes in $VCP^{R155H/+}$ heterozygotes mice

The availability of lysosomal enzymes is necessary for the successful degradation of proteins via the autophagy-lysosomal pathway. To evaluate the effects of increasing percentages of LEDs (12%, 30%, and 48%) on the lysosomal enzyme pathway, we performed Western blot analyses (Fig 5A). We found that levels of the acid phosphatase were significantly decreased in $VCP^{R155H/+}$ mice (either ND or 9% LED) as compared to their WT littermates (Fig 5A).

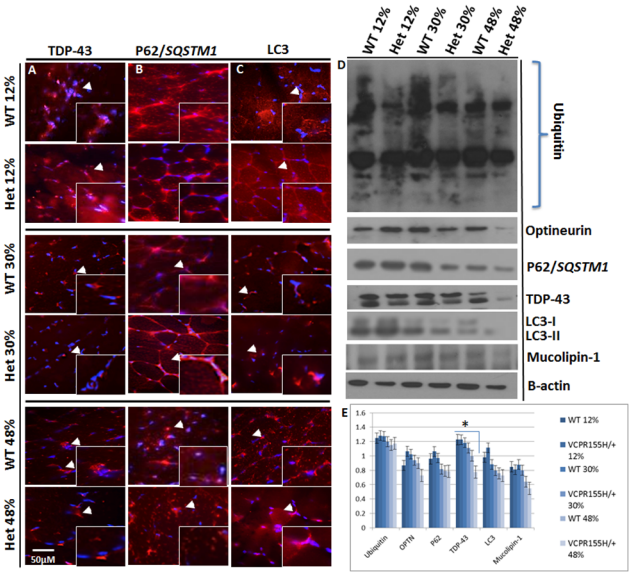

Fig 4. Autophagy influx in the quadriceps of WT and VCP$^{R155H/+}$ mice on normal and different lipid-enriched diets. Immunohistochemical histological analyses comparing WT and heterozygote VCP$^{R155H/+}$ knock-in animals on varying 12%, 30%, and 48% lipid-enriched diets stained with (A) TDP-43 (white arrows), (B) p62/*SQSTM1*, and (C) LC3-I/II. (D) Western blot of WT and heterozygote VCP$^{R155H/+}$ knock-in animals on varying 12%, 30%, and 48% lipid-enriched diets analyzed for ubiquitin, optineurin, p62/*SQSTM1*, TDP-43, LC3-I/II, and Mucolipin (TRPML1). Magnified insets and white arrows indicate increased p62/SQSTM1 autophagic puncta, LC3 and TDP-43 protein expression translocated from the nucleus to the cytoplasm. (E) Densitometry analyses relative to loading control (Beta-actin). Statistical significance is denoted by *P $\leq$ 0.05. The number of mice analyzed per experiment is 8–10.

doi:10.1371/journal.pone.0131995.g004

Interestingly, the VCP$^{R155H/+}$ and WT mice on the 48% LED depicted decreased expression levels of acid phosphatase (Fig 5A). However, we determined that the lysosomal acid lipase (LAL) protein expression in the VCP quadriceps' lysates was unaffected on the ND or on the LEDs (Fig 5A). Densitometry analyses confirmed these Western results (Fig 5B and 5C).

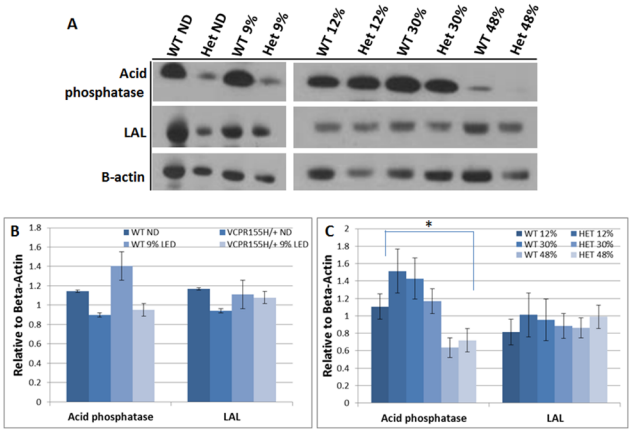

Fig 5. Effects of LED on the expression of lysosomal enzymes in the quadriceps of WT and VCP$^{R155H/+}$ mice on normal and different lipid-enriched diets. (A) Western blot analyses of protein expression levels of acid phosphatase, lysosomal acid lipase in WT and VCP$^{R155H/+}$ knock-in animals on varying ND (6%), 9%, 12%, 30%, and 48% lipid-enriched diets (LED). (B,C) Densitometry analyses of acid phosphatase and LAL from various diets relative to loading control (Beta-actin). Statistical significance is denoted by *P $\leq$ 0.05. The number of mice analyzed per experiment is 8–10.

doi:10.1371/journal.pone.0131995.g005

Discussion

Several studies have previously demonstrated that high fat diets (HFDs) provide powerful therapeutic platforms for many diverse neurological disorders including Alzheimer's disease (AD), Parkinson disease (PD), multiple sclerosis (MS), ALS, and epilepsies [25–30]. Many studies have also shown improvement of neurological deficits, skeletal muscle homeostasis, regulation of autophagy flux, and a reduction of mitochondrial myopathies in mice fed a LED [31–33]. One such study investigated the effects of ketogenic diet (KD) on the features of children with drug therapy-resistant epilepsy and found that KD significantly reduces the frequency of epileptic discharges and demonstrates good clinical efficacy [34]. Similarly, another investigation examining the effects of KD in patients with argininosuccinate lyase (ASL) deficiency showed no metabolic derangement and was well tolerated in patients treated with a protein restriction [35]. Moreover, recent studies using animal models have also shown the neuroprotective properties of KD [36, 37].

In our previous investigation, we discovered that a diet with 2.5% increased lipids (9% LED) reversed the lethal phenotype of the $VCP^{R155H/R155H}$ homozygote animals with significantly improved muscle and bone pathology, motor activity as well as myopathic and mitochondrial staining at three weeks of age [21]. Remarkably, we were able to reverse the lethal phenotype, death by 21 days of age, and increase the survival rate in $VCP^{R155H/R155H}$ mice to over one year, by placing pregnant dams on a 9% LED. Homozygous $VCP^{R155H/R155H}$ animals showed normal histology of quadriceps muscle fibers, increased muscle strength and a slower progression of the disease in the survivors on the LED [21]. However, the LED did not prevent fatal progression of the disease in the mutant $VCP^{R155H/R155H}$ mice [21]. Therefore, we hypothesized that further increasing lipids in the mouse diet may lead to increased amelioration of the VCP pathological phenotypes. In this report, we investigated the progressive course of the homozygous and heterozygote phenotype by monitoring the muscle strength, quadriceps muscles and autophagy dysfunction in animals on normal and increasing lipid-enriched diets (9%, 12%, 30%, and 48%).

To understand the pivotal role of the LEDs in VCP disease, we determined their effects on our novel mouse models: $VCP^{R155H/R155H}$ and $VCP^{R155H/+}$ mice. Initially, we investigated the effects of 9% LED, to uncover if the diet would have any benefit to the heterozygote mice. Our heterozygote mice display the typical phenotypical features as observed in patients, with a point mutation in one allele and later onset of disease, typically 6-months of age, becoming severe around 15-months of age [23]. When we placed one VCP heterozygote cohort on a 9% LED from birth and one cohort from 7 months of age, we found the VCP heterozygote mice, just like the homozygote mice had delayed onset of muscle pathology. Benefits included increased muscle strength and decreased pathology in both animal cohorts. However, the benefit was more pronounced from birth than 7-months of age. This finding suggests genetic screening of families with VCP pathology and early intervention may provide the best clinical outcomes for patients.

Subsequently, we examined the effects of increased lipid diet content on amelioration of muscle pathology in VCP-associated disease. To our surprise, we found that placing mice on a diet regimen with increased lipid-enriched diets (12%, 30%, and 48%) had detrimental effects on survival and muscle pathology of the homozygotes and heterozygote mice. H&E staining of the 15-month old heterozygote $VCP^{R155H/+}$ animals displayed centrally localized nuclei and increased endomysial space between the fibers of muscle quadriceps. 15-month old heterozygote $VCP^{R155H/+}$ mice on the 30% and 48% LEDs revealed decreased strength while no differences were observed in 12% LEDs when compared to age- and sex-matched heterozygote $VCP^{R155H/+}$ mice on ND. Rotarod performance measurements depicted decreased motor

coordination in $VCP^{R155H/+}$ mice on 30% and 48% LEDs. Interestingly, no significant correlation was found between the weights and grip strength and Rotarod measurements in these mice ($P > 0.05$). The relationship between obesity and strength and Rotarod performance measurements will be further investigated in a future study and the results will be the subject of a future report.

These findings could potentially suggest compromised skeletal muscle homeostasis, and impaired mitochondrial metabolism and autophagy-lysosomal pathways. Autophagy is a critical catabolic process necessary for cell growth, development and homeostatic levels of cellular products, and more recently a role in regulating glucose metabolism has been identified. Evidence suggests a molecular link between autophagy and cellular metabolism [38, 39], and thus is important in times of survival during fasting and for reprogramming of cell metabolism [39].

Studies have demonstrated the importance of autophagy in maintaining protein homeostasis and quality control of cellular milieu. However, mechanisms underlying neurodegeneration due to autophagy dysfunction remain unknown. In our study, heterozygous mice placed on increasing diets (12%, 30%, and 48%) showed quadriceps muscle pathology, suggesting autophagy dysfunction and a potential autophagolysosome block. Furthermore, the $VCP^{R155H/+}$ animals on increasing LED demonstrated comparable ubiquitin and TDP-43 levels, but decreased expression levels of p62/*SQSTM1* and LC3 autophagy intermediates in the quadriceps muscles when compared to $VCP^{R155H/+}$ animals on a normal diet. The $VCP^{R155H/+}$ animals on the 48% LED illustrated a slight decrease in the level of expression of TRPML1 protein, suggestive of increased of lipid accumulation, leading to a block in lysosomal trafficking. A study by Shen et al. (2012) demonstrated that increases in the level of expression of TRPML1 protein leads to lipid accumulation and correction of the block in lysosomal trafficking [40]. Similarly, a more recent study by Cheng et al. (2014) showed TRPML1 is required for membrane repair in skeletal muscle to prevent muscular dystrophy [41]. Interestingly, we observed lipid accumulation in the 30% and 48% WT and $VCP^{R155H/+}$ mice quadriceps, suggestive of increased lipotoxicity, thereby resulting in an autophagolysosomal block in the autophagy cascade. Additionally, these animals depicted increased levels of acid phosphatase and LAL, thereby suggesting an interesting relationship in the functionality of the autophagy-lysosomal cascade in VCP disease.

In conclusion, the ability of a fine balance of LEDs to potentially provide a protective effect against fatty acid-induced lipotoxicity and therapeutic effects may allow various mechanisms of repair and growth of skeletal muscle tissue. However, it seems likely that other mechanism systems, such as modification of autophagy and mitophagy, may also play a role in the prolonged survival and improved pathology of the homozygous $VCP^{R155H/R155H}$ and heterozygous $VCP^{R155H/+}$ mice. We speculate that the decrease in autophagy, acid phosphatase and LAL markers may also represent an adaptive mechanism in the presence of increasing fats to degrade proteins. The present findings using the *in vivo* model offer the prospect of elucidating the pathophysiological mechanisms and clinical translation to novel therapies to treat patients with VCP and associated neurodegenerative diseases. Further dissection of the lipid metabolism and its association to autophagic, metabolic, mitophagic signaling transduction pathways are required and could provide insights for future therapeutic clinical applications.

Author Contributions

Conceived and designed the experiments: KJL VEK AN. Performed the experiments: KJL CN NW BT AN. Analyzed the data: KJL LB VEK AN. Contributed reagents/materials/analysis tools: VEK AN. Wrote the paper: KJL LB VEK AN.

References

1. Nalbandian A, Donkervoort S, Dec E, Badadani M, Katheria V, Rana P, et al. The multiple faces of valosin-containing protein-associated diseases: inclusion body myopathy with Paget's disease of bone, frontotemporal dementia, and amyotrophic lateral sclerosis. J Mol Neurosci. 2011; 45(3):522–31. Epub 2011/09/06. doi: 10.1007/s12031-011-9627-y PMID: 21892620.
2. Kimonis VE, Kovach MJ, Waggoner B, Leal S, Salam A, Rimer L, et al. Clinical and molecular studies in a unique family with autosomal dominant limb-girdle muscular dystrophy and Paget disease of bone. Genet Med. 2000; 2(4):232–41. PMID: 11252708.
3. Kovach MJ, Ruiz J, Kimonis K, Mueed S, Sinha S, Higgins C, et al. Genetic heterogeneity in autosomal dominant essential tremor. Genet Med. 2001; 3(3):197–9. PMID: 11388761.
4. Watts GD, Thorne M, Kovach MJ, Pestronk A, Kimonis VE. Clinical and genetic heterogeneity in chromosome 9p associated hereditary inclusion body myopathy: exclusion of GNE and three other candidate genes. Neuromuscul Disord. 2003; 13(7–8):559–67. PMID: 12921793.
5. Kimonis VE, Mehta SG, Fulchiero EC, Thomasova D, Pasquali M, Boycott K, et al. Clinical studies in familial VCP myopathy associated with Paget disease of bone and frontotemporal dementia. American journal of medical genetics. 2008; 146(6):745–57. PMID: 18260132.
6. Watts GD, Wymer J, Kovach MJ, Mehta SG, Mumm S, Darvish D, et al. Inclusion body myopathy associated with Paget disease of bone and frontotemporal dementia is caused by mutant valosin-containing protein. Nature genetics. 2004; 36(4):377–81. PMID: 15034582.
7. Kimonis VE, Fulchiero E, Vesa J, Watts G. VCP disease associated with myopathy, paget disease of bone and frontotemporal dementia: Review of a unique disorder. Biochimica et biophysica acta. 2008. PMID: 18845250.
8. Ju JS, Weihl CC. Inclusion body myopathy, Paget's disease of the bone and fronto-temporal dementia: a disorder of autophagy. Human molecular genetics. 2010; 19(R1):R38–45. PMID: 20410287. doi: 10.1093/hmg/ddq157
9. Ju JS, Fuentealba RA, Miller SE, Jackson E, Piwnica-Worms D, Baloh RH, et al. Valosin-containing protein (VCP) is required for autophagy and is disrupted in VCP disease. The Journal of cell biology. 2009; 187(6):875–88. PMID: 20008565. doi: 10.1083/jcb.200908115
10. Vesa J, Su H, Watts GD, Krause S, Walter MC, Martin B, et al. Valosin containing protein associated inclusion body myopathy: abnormal vacuolization, autophagy and cell fusion in myoblasts. Neuromuscul Disord. 2009; 19(11):766–72. PMID: 19828315. doi: 10.1016/j.nmd.2009.08.003
11. Nalbandian A, Ghimbovschi S, Radom-Aizik S, Dec E, Vesa J, Martin B, et al. Global Gene Profiling of VCP-associated Inclusion Body Myopathy. Clin Transl Sci. 2012; 5(3):226–34. Epub 2012/06/13. doi: 10.1111/j.1752-8062.2012.00407.x PMID: 22686199; PubMed Central PMCID: PMC3375869.
12. Lee HS, Daniels BH, Salas E, Bollen AW, Debnath J, Margeta M. Clinical utility of LC3 and p62 immunohistochemistry in diagnosis of drug-induced autophagic vacuolar myopathies: a case-control study. PLoS ONE. 2012; 7(4):e36221. Epub 2012/05/05. doi: 10.1371/journal.pone.0036221 PONE-D-11-25789 [pii]. PMID: 22558391; PubMed Central PMCID: PMC3338695.
13. Tung YT, Wang BJ, Hu MK, Hsu WM, Lee H, Huang WP, et al. Autophagy: a double-edged sword in Alzheimer's disease. J Biosci. 2012; 37(1):157–65. Epub 2012/02/24. PMID: 22357213.
14. Heng MY, Detloff PJ, Paulson HL, Albin RL. Early alterations of autophagy in Huntington disease-like mice. Autophagy. 2010; 6(8):1206–8. Epub 2010/10/12. doi: 13617 [pii]. PMID: 20935460; PubMed Central PMCID: PMC3039724.
15. Shea L, Raben N. Autophagy in skeletal muscle: implications for Pompe disease. International journal of clinical pharmacology and therapeutics. 2009; 47 Suppl 1:S42–7. PMID: 20040311.
16. Lunemann JD, Schmidt J, Dalakas MC, Munz C. Macroautophagy as a pathomechanism in sporadic inclusion body myositis. Autophagy. 2007; 3(4):384–6. PMID: 17438365.
17. Nalbandian A, Llewellyn K, Badadani M, Yin H, Nguyen C, Katheria V, et al. A Progressive Translational Mouse Model of Human VCP Disease: The VCP R155H/+ Mouse. Muscle & nerve. 2012;(in press).
18. Yin HZ, Nalbandian A, Hsu CI, Li S, Llewellyn KJ, Mozaffar T, et al. Slow development of ALS-like spinal cord pathology in mutant valosin-containing protein gene knock-in mice. Cell Death Dis. 2012; 3: e374. Epub 2012/08/18. doi: cddis2012115 [pii] doi: 10.1038/cddis.2012.115 PMID: 22898872; PubMed Central PMCID: PMC3434652.
19. Nalbandian A, Llewellyn KJ, Kitazawa M, Yin HZ, Badadani M, Khanlou N, et al. The homozygote VCP (R(1)(5)(5)H/R(1)(5)(5)H) mouse model exhibits accelerated human VCP-associated disease pathology. PLoS ONE. 2012; 7(9):e46308. doi: 10.1371/journal.pone.0046308 PMID: 23029473; PubMed Central PMCID: PMC3460820.

20. Nalbandian A, Llewellyn KJ, Kitazawa M, Yin HZ, Badadani M, Khanlou N, et al. The Homozygote VCP (R155H/R155H) Mouse Model Exhibits Accelerated Human VCP-Associated Disease Pathology. PLoS ONE. 2012; 7(9):e46308. Epub 2012/10/03. doi: 10.1371/journal.pone.0046308 PONE-D-12-17339 [pii]. PMID: 23029473; PubMed Central PMCID: PMC3460820.

21. Llewellyn KJ, Nalbandian A, Jung KM, Nguyen C, Avanesian A, Mozaffar T, et al. Lipid-enriched diet rescues lethality and slows down progression in a murine model of VCP-associated disease. Human molecular genetics. 2014; 23(5):1333–44. doi: 10.1093/hmg/ddt523 PMID: 24158850; PubMed Central PMCID: PMC3919004.

22. Badadani M, Nalbandian A, Watts GD, Vesa J, Kitazawa M, Su H, et al. VCP associated inclusion body myopathy and paget disease of bone knock-in mouse model exhibits tissue pathology typical of human disease. PLoS ONE. 2010; 5(10). Epub 2010/10/20. doi: 10.1371/journal.pone.0013183 PMID: 20957154; PubMed Central PMCID: PMC2950155.

23. Nalbandian A, Llewellyn KJ, Badadani M, Yin HZ, Nguyen C, Katheria V, et al. A progressive translational mouse model of human valosin-containing protein disease: the VCP(R155H/+) mouse. Muscle & nerve. 2013; 47(2):260–70. doi: 10.1002/mus.23522 PMID: 23169451; PubMed Central PMCID: PMC3556223.

24. Nalbandian A, Nguyen C, Katheria V, Llewellyn KJ, Badadani M, Caiozzo V, et al. Exercise training reverses skeletal muscle atrophy in an experimental model of VCP disease. PLoS ONE. 2013; 8(10): e76187. doi: 10.1371/journal.pone.0076187 PMID: 24130765; PubMed Central PMCID: PMC3794032.

25. Baranano KW, Hartman AL. The ketogenic diet: uses in epilepsy and other neurologic illnesses. Curr Treat Options Neurol. 2008; 10(6):410–9. Epub 2008/11/08. PMID: 18990309; PubMed Central PMCID: PMC2898565.

26. Evangeliou A, Vlachonikolis I, Mihailidou H, Spilioti M, Skarpalezou A, Makaronas N, et al. Application of a ketogenic diet in children with autistic behavior: pilot study. Journal of child neurology. 2003; 18 (2):113–8. Epub 2003/04/16. PMID: 12693778.

27. Gasior M, Rogawski MA, Hartman AL. Neuroprotective and disease-modifying effects of the ketogenic diet. Behav Pharmacol. 2006; 17(5–6):431–9. Epub 2006/08/31. doi: 00008877-200609000-00009 [pii]. PMID: 16940764; PubMed Central PMCID: PMC2367001.

28. Jozwiak S, Kossoff EH, Kotulska-Jozwiak K. Dietary treatment of epilepsy: rebirth of an ancient treatment. Neurol Neurochir Pol. 2011; 45(4):370–8. Epub 2011/11/22. doi: 17519 [pii]. PMID: 22101998.

29. Siva N. Can ketogenic diet slow progression of ALS? Lancet Neurol. 2006; 5(6):476. Epub 2006/06/03. PMID: 16739298.

30. Stafstrom CE, Rho JM. The ketogenic diet as a treatment paradigm for diverse neurological disorders. Front Pharmacol. 2012; 3:59. Epub 2012/04/18. doi: 10.3389/fphar.2012.00059 PMID: 22509165; PubMed Central PMCID: PMC3321471.

31. Camargo N, Brouwers JF, Loos M, Gutmann DH, Smit AB, Verheijen MH. High-fat diet ameliorates neurological deficits caused by defective astrocyte lipid metabolism. FASEB J. 2012. Epub 2012/07/04. doi: fj.12-205807 [pii] doi: 10.1096/fj.12-205807 PMID: 22751013.

32. Moresi V, Carrer M, Grueter CE, Rifki OF, Shelton JM, Richardson JA, et al. Histone deacetylases 1 and 2 regulate autophagy flux and skeletal muscle homeostasis in mice. Proceedings of the National Academy of Sciences of the United States of America. 2012; 109(5):1649–54. Epub 2012/02/07. doi: 1121159109 [pii] doi: 10.1073/pnas.1121159109 PMID: 22307625; PubMed Central PMCID: PMC3277131.

33. Turner N, Bruce CR, Beale SM, Hoehn KL, So T, Rolph MS, et al. Excess lipid availability increases mitochondrial fatty acid oxidative capacity in muscle: evidence against a role for reduced fatty acid oxidation in lipid-induced insulin resistance in rodents. Diabetes. 2007; 56(8):2085–92. Epub 2007/05/24. doi: db07-0093 [pii] doi: 10.2337/db07-0093 PMID: 17519422.

34. Li B, Tong L, Jia G, Sun R. Effects of ketogenic diet on the clinical and electroencephalographic features of children with drug therapy-resistant epilepsy. Experimental and therapeutic medicine. 2013; 5 (2):611–5. doi: 10.3892/etm.2012.823 PMID: 23404539; PubMed Central PMCID: PMC3570117.

35. Peuscher R, Dijsselhof ME, Abeling NG, Van Rijn M, Van Spronsen FJ, Bosch AM. The ketogenic diet is well tolerated and can be effective in patients with argininosuccinate lyase deficiency and refractory epilepsy. JIMD reports. 2012; 5:127–30. doi: 10.1007/8904_2011_115 PMID: 23430928; PubMed Central PMCID: PMC3509918.

36. Luan G, Zhao Y, Zhai F, Chen Y, Li T. Ketogenic diet reduces Smac/Diablo and cytochrome c release and attenuates neuronal death in a mouse model of limbic epilepsy. Brain Res Bull. 2012; 89(3–4):79–85. doi: 10.1016/j.brainresbull.2012.07.002 PMID: 22796483.

37. Noh HS, Kim YS, Choi WS. Neuroprotective effects of the ketogenic diet. Epilepsia. 2008; 49 Suppl 8:120–3. doi: 10.1111/j.1528-1167.2008.01855.x PMID: 19049608.

38. Rabinowitz JD, White E. Autophagy and metabolism. Science (New York, NY. 2010; 330(6009):1344–8. Epub 2010/12/04. doi: 330/6009/1344 [pii] doi: 10.1126/science.1193497 PMID: 21127245; PubMed Central PMCID: PMC3010857.

39. Schiaffino S, Mammucari C, Sandri M. The role of autophagy in neonatal tissues: just a response to amino acid starvation? Autophagy. 2008; 4(5):727–30. Epub 2008/04/26. doi: 6143 [pii]. PMID: 18437051.

40. Shen D, Wang X, Li X, Zhang X, Yao Z, Dibble S, et al. Lipid storage disorders block lysosomal trafficking by inhibiting a TRP channel and lysosomal calcium release. Nature communications. 2012; 3:731. doi: 10.1038/ncomms1735 PMID: 22415822; PubMed Central PMCID: PMC3347486.

41. Cheng X, Zhang X, Gao Q, Ali Samie M, Azar M, Tsang WL, et al. The intracellular Ca(2)(+) channel MCOLN1 is required for sarcolemma repair to prevent muscular dystrophy. Nature medicine. 2014; 20 (10):1187–92. doi: 10.1038/nm.3611 PMID: 25216637; PubMed Central PMCID: PMC4192061.